

# Quasar catalogue for the astrometric calibration of the forthcoming ILMT survey

Amit Kumar Mandal<sup>1,4</sup>, Bikram Pradhan<sup>2</sup>, Jean Surdej<sup>3</sup>, C. S. Stalin<sup>4</sup>, Ram Sagar<sup>4</sup>, Blesson Mathew<sup>1</sup>

<sup>1</sup>Department of Physics, CHRIST (Deemed to be University), Hosur Road, Bangalore 560029, India.

<sup>2</sup>Aryabhata Research Institute of Observational Sciences, Manora Peak, Nainital 263001, India.

<sup>3</sup>Space science, Technologies and Astrophysics Research (STAR) Institute, Université de Liège, Allée du 6 Août 19c, 4000 Liège, Belgium.

<sup>4</sup>Indian Institute of Astrophysics, Block II, Koramangala, Bangalore, 560034, India.

\*Corresponding author. E-mail: amitkumar@iiap.res.in

MS received 27 May 2020; accepted 13 July 2020

**Abstract.** Quasars are ideal targets to use for astrometric calibration of large scale astronomical surveys as they have negligible proper motion and parallax. The forthcoming 4-m International Liquid Mirror Telescope (ILMT) will survey the sky that covers a width of about  $27'$ . To carry out astrometric calibration of the ILMT observations, we aimed to compile a list of quasars with accurate equatorial coordinates and falling in the ILMT stripe. Towards this, we cross-correlated all the quasars that are known till the present date with the sources in the *Gaia*-DR2 catalogue, as the *Gaia*-DR2 sources have position uncertainties as small as a few milli arcsec (*mas*). We present here the results of this cross-correlation which is a catalogue of 6738 quasars that is suitable for astrometric calibration of the ILMT fields. In this work, we present this quasar catalogue. This catalogue of quasars can also be used to study quasar variability over diverse time scales when the ILMT starts its observations. While preparing this catalogue, we also confirmed that quasars in the ILMT stripe have proper motion and parallax lesser than  $20 \text{ mas yr}^{-1}$  and  $10 \text{ mas}$ , respectively.

**Keywords.** quasars—parallaxes—proper motions—ILMT—astrometry.

## 1. Introduction

The 4 m International Liquid Mirror Telescope (ILMT) which will observe in the Time Delayed Integration (TDI) mode is expected to be commissioned soon on the Aryabhata Research Institute of Observational Sciences (ARIES) site in Devasthal, India (Surdej et al. 2018). The ILMT will be repeatedly scanning the sky within a narrow stripe of width  $\sim 27'$ . The positions of the celestial objects in the sky change with time as the sky moves across the fixed detector surface due to the rotation of the Earth around the polar axis. The TDI mode of the charge couple device (CCD) mounted at the ILMT helps to track the stars by registering the electronic charges with the rate at which the target source drifts across the detector (Surdej et al. 2018) and the positions of each object in the observed image come out in pixel units. To convert the observations from the pixel coordinate system to the world coordinate system ( $\alpha, \delta$ ) we need to carry out astrometric calibration of the ILMT fields. For that, we choose quasars as astromet-

ric standards because of their negligible proper motions (PM) and trigonometric parallaxes.

The number of quasars we know as of today has significantly increased since their first identification about six decades ago (Schmidt 1963). This increase is mainly due to large surveys such as the Two degree Field (2dF) QSO survey (Croom et al. 2004) in the southern sky and the Sloan Digital Sky Survey (SDSS) in the northern sky (Abolfathi et al. 2018, Pâris et al. 2018). Quasars known from different surveys are also gathered and put together in the form of catalogues, through several releases by Véron-Cetty & Véron (2006, 2010) and the Million Quasars (Milliquas) catalogue by Flesch (2017). These catalogues have quasars from different origins with different accuracies in their optical positions. But these catalogues do not provide the errors associated with the equatorial coordinate positions as well as other information such as parallax and PM. Therefore, quasars taken from these catalogues cannot be directly used as sources to carry out astrometric calibration.

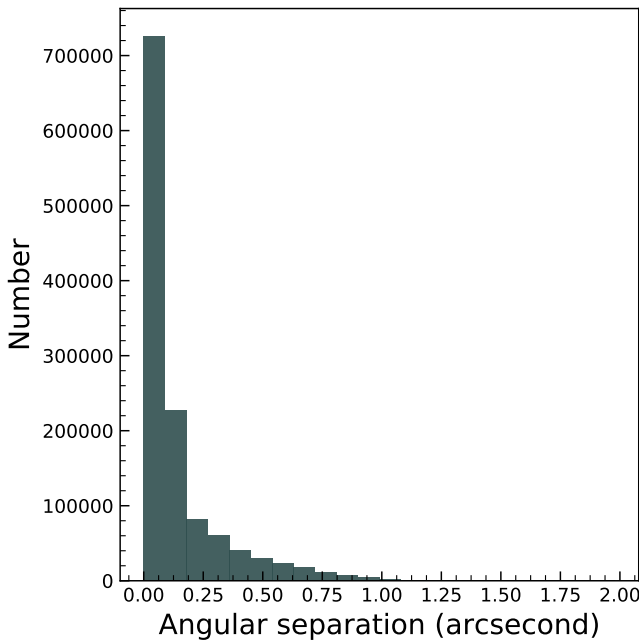


**Figure 1.** Distribution of the angular separation between the quasars in the Million Quasars catalogue and their counterparts in *Gaia*-DR2.

The main motivation of the present work is therefore to construct a catalogue of quasars that will be used to carry out astrometric calibration of the ILMT fields by including (i) more precise positions of the sources with uncertainties, (ii) additional important information such as parallax and PM and, (iii) the photometry of the objects. We describe the data used in this work in Section 2. The procedures followed to make the quasar catalogue and the outcome is presented in Section 3. Applications of the catalogue are discussed in Section 4 followed by the Summary in the final Section.

## 2. Data used

To select a catalogue of quasars suitable for astrometric calibration of the ILMT observations we need to consider all quasars we know as of today. This can come from a wide variety of surveys carried out at different wavelengths such as optical, infrared, radio, etc. One such quasar catalogue suited for our purpose is the Milliquas catalogue. This is the largest compilation of quasars we have as of today. This catalogue contains about 1998464 quasars taken from all the quasar surveys available in the literature. The majority of quasars in the Milliquas catalogue comes from the SDSS, one of the ambitious sky surveys covering more than a quarter of the sky in the northern hemisphere in five optical

filters. Other quasars included in Milliquas are from the NBCKDE, NBCKDE-v3 (Richards et al. 2009, 2015), XDQSO (Bovy et al. 2011; Myers et al. 2015), AllWISE and Peters photometric quasar catalogues (Peters et al. 2015) as well as quasars from all-sky radio/X-ray surveys. As the Milliquas catalogue is a compilation of various quasar surveys, it has varied uncertainties in the equatorial coordinates. For astrometric calibration, one needs to have quasars with precise positions. A source that provides precise positions of celestial sources is the survey being presently carried out by the European Space Agency *Gaia* mission. *Gaia*-DR2 (Lindgren et al. 2018, Gaia Collaboration et al. 2018) contains data from the all sky astrometric and photometric survey conducted by *Gaia* and provides accurate positions for about 1.7 billion sources, with PM and parallax measurements for about 1.3 billion sources (Marrese et al. 2019). Therefore, to get accurate positions for the quasars in the Milliquas catalogue we used the precise and homogeneous measurements from *Gaia*-DR2.

## 3. Methods followed and the resulting catalogue

It is known that quasars represent quasi-ideal astrometric reference sources over the celestial sphere because of their negligible PM and are thus suitable candidates for use to carry out astrometric calibration (Souhay et al. 2015) of the ILMT survey. We therefore aim to gather accurate position, PM and trigonometric parallax for all quasars available in the Milliquas catalogue from the *Gaia*-DR2 database and then select a sub-set of them for the ILMT use. To calculate the absolute or resultant PM  $\mu$  we used the relation given by Varshni (1982)

$$\mu = (\mu_{\alpha}^2 \cos^2 \delta + \mu_{\delta}^2)^{1/2} \quad (1)$$

where  $\alpha$  and  $\delta$  are the right ascension (RA) and declination (DEC) respectively. We collected  $\mu_{\alpha} \cos \delta$  and  $\mu_{\delta}$  values from the *Gaia*-DR2 database. The error in  $\mu$  was calculated using the standard error propagation method. To arrive at a separate list of quasars for the ILMT field of view (FoV), we followed the following steps:

1. We cross-correlated nearly 2 million objects in the Milliquas catalogue with *Gaia*-DR2 with angular proximity of less than 2". We used a 2" angular separation because a large fraction of the objects in the Milliquas catalogue are from SDSS that has imaging data with seeing less than 2" (Ross et al. 2011). By cross-correlating the

**Table 1.** The ILMT Quasar (IQ) catalogue. The details on each column of this table is given in Table 2. The full catalogue is available in the electronic version of the article.

ID-1 (1)*	RA (2)*	RA-ERR (3)*	DEC (4)*	DEC-ERR (5)*	<i>z</i> (6)	...	...	PM-DEC (16)*	PM-DECERR (17)*	EPSILON (18)	D (19)
2.85518e+18	0.06120	0.54785	29.23513	0.28529	1.90	...	...	1.31259	0.50398	0.00	0.00
2.85525e+18	0.07183	0.22781	29.50171	0.15339	1.40	...	...	0.27730	0.26071	0.00	0.00
2.85525e+18	0.10806	0.62917	29.50235	0.56513	2.51	...	...	-1.02912	1.06549	1.44	0.87

\*The values are up to 5 decimal places, the original values retrieved from the *Gaia*-DR2 catalogue are mentioned in the IQ catalogue available in the electronic version of the article.

**Table 2.** Column information of the ILMT Quasar (IQ) catalogue.

Number	Column Name	Format	Unit	Description
1	ID-1	String		Object name as given in <i>Gaia</i> -DR2
2	RA	Double	degree	Right Ascension (J2000)
3	RA-ERR	Double	<i>mas</i>	Error in Right Ascension retrieved from <i>Gaia</i> -DR2
4	DEC	Double	degree	Declination (J2000)
5	DEC-ERR	Double	<i>mas</i>	Error in Declination retrieved from <i>Gaia</i> -DR2
6	<i>z</i>	Double		Redshift
7	ID-2	String		Object ID in the Milliquas catalogue
8	TYPE	String		Classification of the object
9	PROB	Double		Probability that the object is a quasar <sup>•</sup>
10	MAG	Double		<i>Gaia</i> G-band magnitude
11	MAG-ERR	Double		Error in <i>Gaia</i> G-band magnitude
12	PLX	Double	<i>mas</i>	Parallax
13	PLX-ERR	Double	<i>mas</i>	Error in parallax
14	PM-RA	Double	<i>mas yr</i> <sup>-1</sup>	Proper motion in RA
15	PM-RAERR	Double	<i>mas yr</i> <sup>-1</sup>	Error in proper motion in RA
16	PM-DEC	Double	<i>mas yr</i> <sup>-1</sup>	Proper motion in DEC
17	PM-DECERR	Double	<i>mas yr</i> <sup>-1</sup>	Error in proper motion in DEC
18	EPSILON	Double		Astrometric excess noise
19	D	Double		Significance of excess noise

<sup>•</sup> The details on how the probability is assigned to each quasar can be found in Flesch (2015).

Milliquas catalogue with the *Gaia*-DR2, we arrived at a sample of 1235600 objects spanning a range of redshifts up to  $z = 6.4$ . The distribution of the angular separation for the matched objects between the position in the Milliquas catalogue and the position in *Gaia*-DR2 is shown in Fig. 1. The distribution has a range between 0 and  $1.97''$  with a mean of  $0.15''$  and a standard deviation of  $0.18''$ . About 99.8% of the objects are matched within  $1''$ . The distributions of  $z$  and G-band brightness of these objects are shown in Fig. 2.

2. Among the many parameters provided by *Gaia*-DR2, two parameters that are relevant for quasar target selection are the astrometric excess noise ( $\epsilon_i$ ) and its significance namely the astrometric excess noise significance (D). Excess noise  $\epsilon_i$  quantifies the disagreement between the observations and the best-fitting standard astrometric model adopted by *Gaia* (Lindgren et al. 2012). A value  $\epsilon_i = 0$  implies that the source is astrometrically well behaved, and a value  $\epsilon_i > 0$  indicates that the residuals are statistically larger than expected. However, practically there is the possibility that some sources may not behave exactly according to the adopted astrometric model. Therefore, the significance of  $\epsilon_i$  is characterised by its significance namely D (Lindgren et al. 2012). If,  $D \leq 2$ ,  $\epsilon_i$  is probably not significant and the source may be astrometrically well-behaved even if  $\epsilon_i$  is large<sup>1</sup>. Therefore, we only selected sources with  $D \leq 2$  from *Gaia*-DR2. This yielded a total of 1047747 quasars covering the whole sky. For these quasars, we calculated PM using Equation 1. The distribution of their PM is shown in Fig. 3. From this figure, it is evident that except for a few objects (about 0.25%) most of them have PM less than  $20 \text{ mas yr}^{-1}$  with a mean value and standard deviation of  $1.808 \text{ mas yr}^{-1}$  and  $2.878 \text{ mas yr}^{-1}$ , respectively.
3. From the list of quasars obtained at step 2 above, we made a separate catalogue of quasars for the ILMT stripe. The Devasthal observatory where the ILMT is being installed is located at a latitude near  $29^\circ 22' 26''$  (Surdej et al. 2018). The width of the ILMT FoV is  $\sim 27'$ . However, the ILMT sky at zenith will change with time due to precession as shown in Fig. 4. It has been found that if we take a  $\sim 34'$  wide stripe instead of  $\sim 27'$ , the effect of precession during the next

10 years will be taken into account. So as *Gaia* has a limiting G-band magnitude of  $21^2$ , we selected only those quasars having a declination ( $\delta$ ) in the range  $29.09^\circ \leq \delta \leq 29.66^\circ$  and G-mag  $\leq 21$  from the sample of 1047747 quasars obtained from step 2 since only these will be accessible for observations with the ILMT. Using the above criteria, we arrived at a sample of 6904 quasars. For slightly less than 2% of these, we do not have the redshift information in the Milliquas catalogue. Excluding those, we arrived at a final catalogue of 6755 quasars available within the ILMT stripe.

4. A plot of the PM of these objects as a function of their G-band brightness is shown in Fig. 5. From this figure, it is evident that the majority of the quasars have  $\text{PM} < 20 \text{ mas yr}^{-1}$ . We only found 17 quasars in this list with  $\text{PM} > 20 \text{ mas yr}^{-1}$  and all of them are fainter than 19.5 mag in the G-band. The nature of these 17 objects could not be ascertained due to the lack of optical spectra for them. Therefore, we neglected those 17 quasars from our list and arrived at a final sample of 6738 quasars that will be visible with the ILMT and could be used as astrometric calibrators.

Varshni (1982) claimed the existence of high PM quasars namely PHL 1033, LB 8956 and LB 8991 with PM values of  $0.049 \pm 0.013$ ,  $0.061 \pm 0.018$  and  $0.050 \pm 0.018 \text{ arcsec yr}^{-1}$  respectively. We checked the PM of these objects in *Gaia*-DR2 and found PM values of  $0.121 \pm 0.435$ ,  $0.188 \pm 0.151$  and  $0.056 \pm 0.072 \text{ mas yr}^{-1}$  for PHL 1033, LB 8956 and LB 8991 respectively. This along with the observations in Fig. 5 point to quasars having  $\text{PM} < 20 \text{ mas yr}^{-1}$ .

5. The distributions of redshifts, G-band magnitude and parallax of the ILMT quasars are illustrated in Fig. 6. They span redshifts up to  $z = 4.9$ . Their distribution in the galactic coordinate system is shown in Fig. 7. The sample catalogue and the description of its columns are given in Table 1 and Table 2, respectively. The full catalogue is available in the electronic version of the present article.

#### 4. Applications of the catalogue

The ILMT will be continuously scanning the sky passing over zenith. Such observations will be of inter-

<sup>1</sup>[https://gea.esac.esa.int/archive/documentation/GDR2/Gaia\\_archive/chap\\_datamodel/sec\\_dm\\_main\\_tables/sssec\\_dm\\_gaia\\_source.html](https://gea.esac.esa.int/archive/documentation/GDR2/Gaia_archive/chap_datamodel/sec_dm_main_tables/sssec_dm_gaia_source.html)

<sup>2</sup><https://www.cosmos.esa.int/web/gaia/dr2>

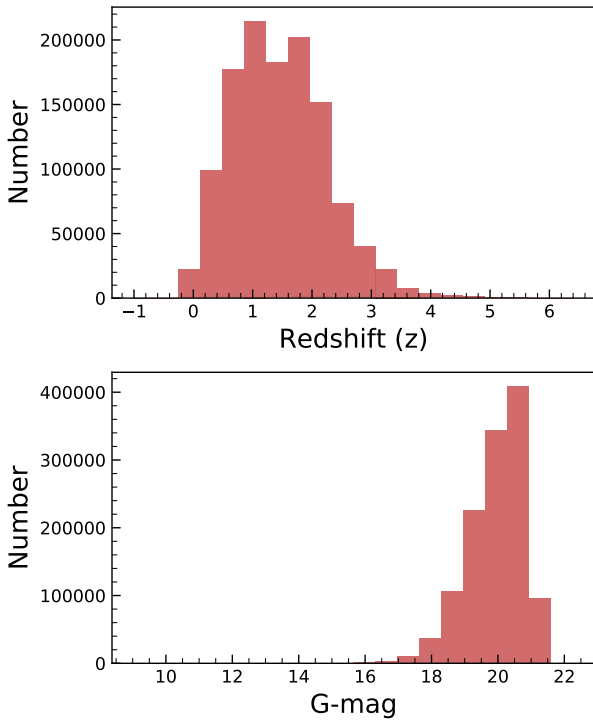


**Figure 2.** Distribution of redshift (top) and *Gaia* G-band magnitude (bottom) of the quasars selected from the Million Quasars catalogue.

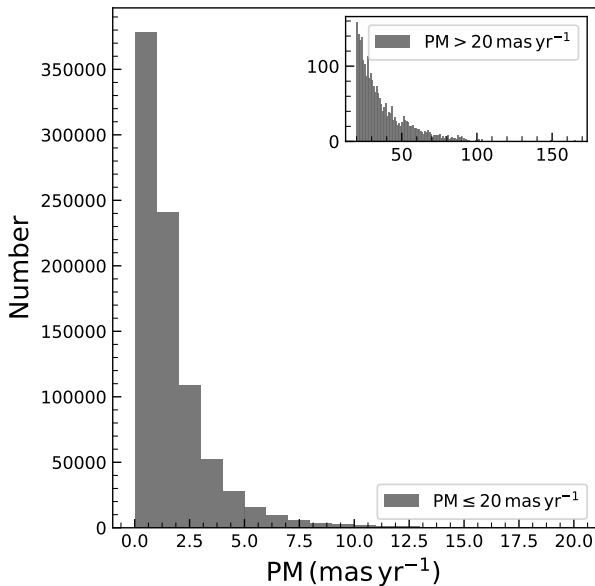


**Figure 3.** Distribution of the PM for quasars in the Million Quasars catalogue with  $D \leq 2$ . There are about 2615 quasars with  $PM > 20 \text{ mas yr}^{-1}$ , their PM distribution is shown in the small box on the same figure.

The maximum deviation of RA or DEC between epoch 2019 and 2029

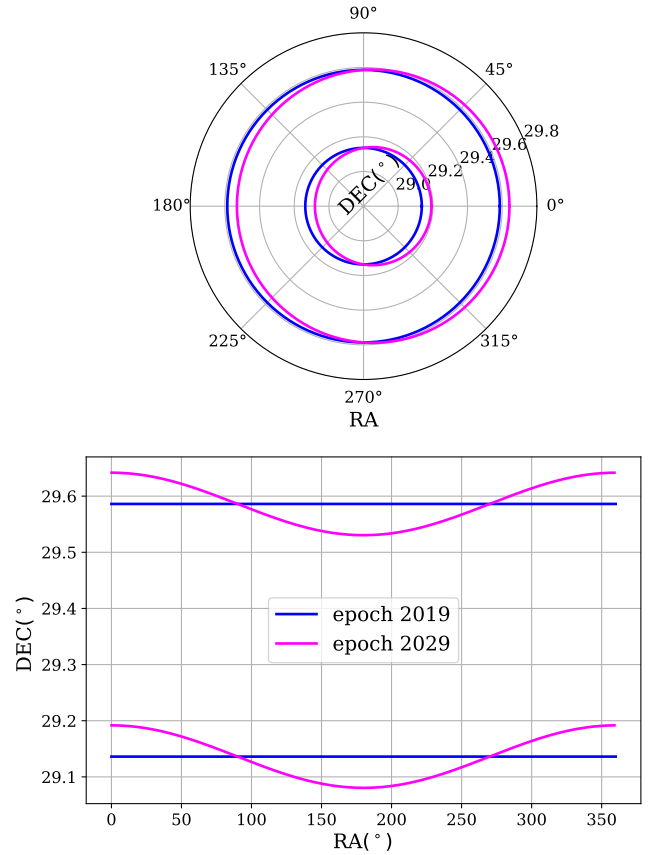


**Figure 4.** (Top) Polar plot showing the astrometric deviation of the ILMT stripe between the 2019 and 2029 epochs due to precession. (Bottom) Deviation in astrometry between the 2019 and 2029 epochs considering that the original ILMT stripe is rectangular in 2019 (blue lines) and pink lines represent the same in 2029.

esting use for a wide range of astrophysical applications such as the detection of many extragalactic objects like supernovae, galaxy clusters, active galactic nuclei (AGN)/quasars, gravitationally lensed systems etc. (Surdej et al. 2018). Also, as zenith region of the sky will be repeatedly scanned by the ILMT, accumulated observations will be very useful for photometric variability studies of different types of celestial sources. As we have already arrived at a catalogue of 6738 quasars that will be covered by the ILMT, we describe below some of the potential applications of this quasar catalogue.

#### 4.1 Astrometric calibration of the ILMT field

The main application of this catalogue of quasars is to calibrate the ILMT observations in the world coordi-

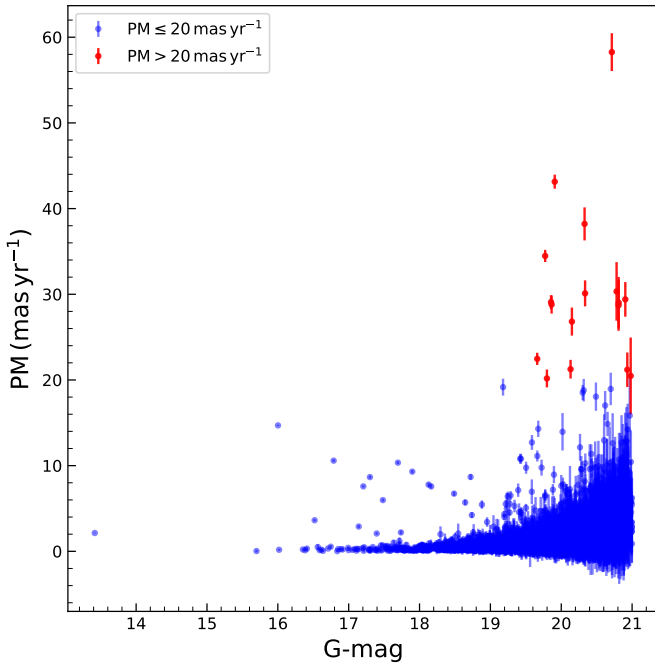


**Figure 5.** Proper motion versus G-mag of the quasars in the ILMT stripe.

nate system. As this catalogue has accurate positions from the *Gaia*-DR2, with errors in the positions of the order of a few *mas*, using these quasars we expect to achieve sub-arcsec astrometric accuracy in the ILMT survey. We performed a Monte Carlo simulation to estimate the astrometric accuracy for the survey. Given the pixel scale of 0.4'' and median seeing at Devasthal observatory of 1.1'' (Sagar et al. 2000; Sagar, Kumar & Omar 2019 and references therein), several synthetic CCD frames were generated having a circular Gaussian point spread function at random locations corresponding to different SDSS *i'* magnitudes assuming a single scan (i.e. exposure time of 102 seconds) as demonstrated by Kumar et al. (2018). The Source Extractor software developed by Barbary (2016) was then used to estimate the centroid of each synthetic source. The  $1\sigma$  accuracy in estimating the centroid of a point source having a limiting *i'* magnitude of 21.4 mag with the 4-m ILMT was found to be 0.09'' (see Fig. 8).

The distribution of the ILMT quasars in RA is shown in Fig. 9. This Figure indicates that ILMT quasars cover the entire range of RA, however for RA between 3–6 hr and between 19–21 hr the numbers of quasars are around 60 and 20 per hr angle in the ILMT field, respectively, much lower than the number of quasars in the other RA ranges. In this range, we have to compromise with a separate database of astrometric standards such as the Tycho-2 catalogue (Hog et al. 2000) which has an astrometric uncertainty of

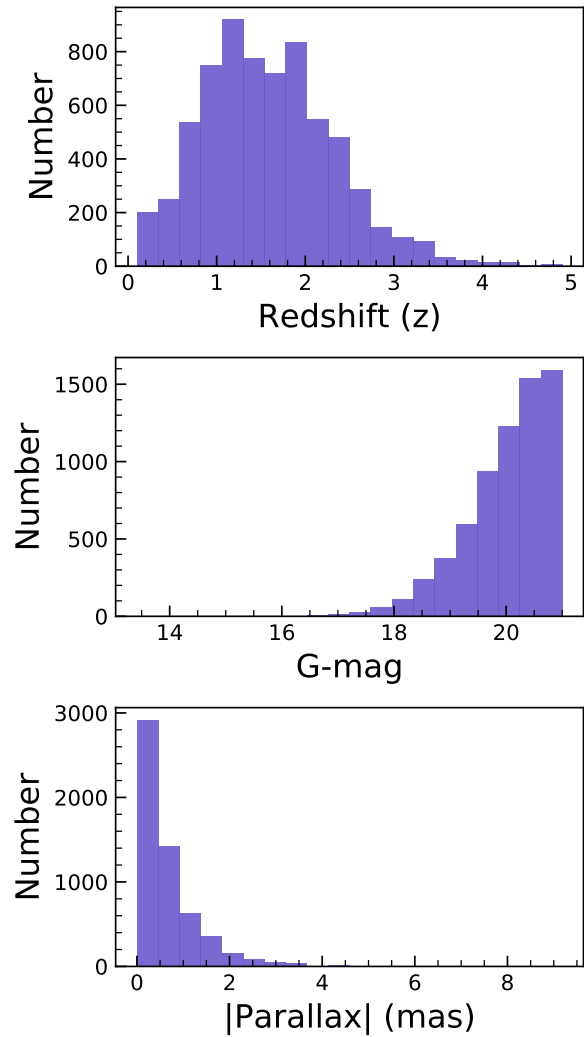


**Figure 6.** Distributions of the redshift, G-band magnitude and absolute parallax of the selected quasars in the ILMT stripe.

0.06'' per coordinate and an average star density of  $\sim 180$  per hr angle. Hence, after adding this uncertainty in quadrature to our estimate the  $1\sigma$  positional accuracy for the faintest stars detectable by ILMT will be degraded to 0.11'' in the aforementioned RA ranges.

#### 4.2 Quasar variability

Optical flux variations in quasars are known since their discovery. They have been studied for optical flux variations over a range of time scales from minutes to days (Wagner & Witzel 1995, Ulrich et al. 1997). Most of the available studies are limited by the time resolution of the observations manifested as gaps in the data. The 4K $\times$ 4K CCD camera mounted on the ILMT can operate over the 4000 to 11000 Å spectral range in three different SDSS equivalent filters *g'*, *r'* and *i'*. The typi-

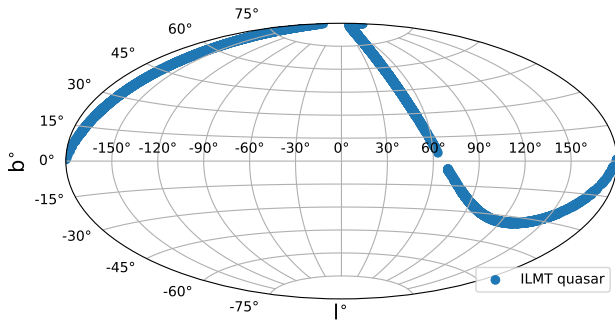


**Figure 7.** Sky distribution of the selected ILMT quasars in the galactic coordinate system. The real surface density of quasars is not considered in this plot.

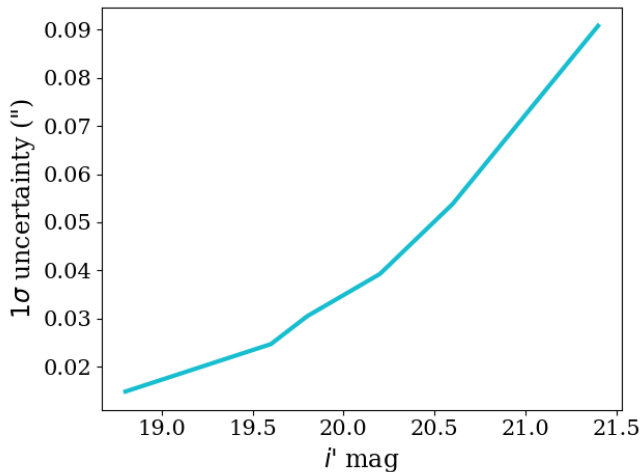


**Figure 8.** Estimation of the  $1\sigma$  uncertainty in the astrometric position of point sources with different magnitudes in the ILMT CCD images.

cal exposure time for a single frame is  $\sim 104$  s (Surdej et al. 2018). Only one of those filters will be used throughout a single night. The observing strategy of the ILMT will enable one to collect good quality data for most of the 6738 quasars that we have arrived at in this work primarily for astrometric calibration. Therefore, the quasars catalogued in this work can be studied for optical flux variability in different optical bands as well as colour variability. When more epochs of observations become available from the ILMT in the future, new candidate quasars can also be discovered based on colour-colour diagram (Richards et al. 2002) as well as optical variability characteristics (Graham et al. 2016).

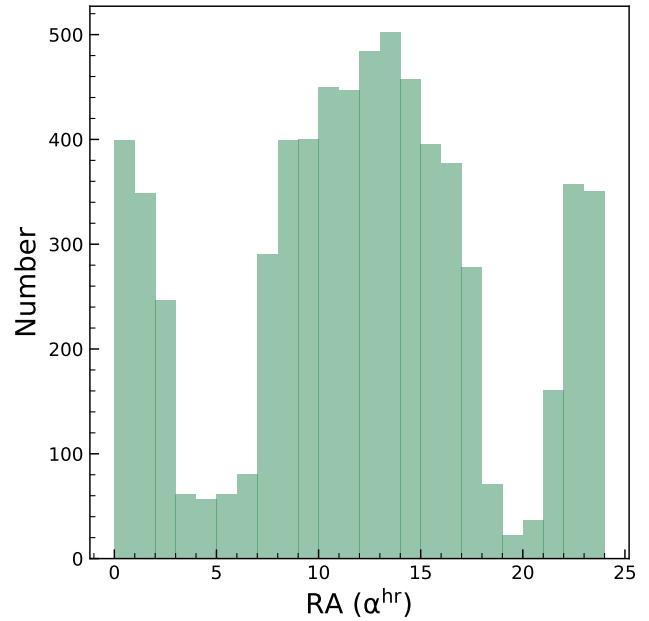


**Figure 9.** Distribution of the selected ILMT quasars in RA.

### 4.3 Variability of lensed quasar

Gravitational lensing, the effect of deflection of light by a foreground intervening compact object (galaxy, cluster, etc.) constitutes a powerful tool that finds applications in many astrophysical areas. Gravitational lensing of distant quasars leads to the formation of multiply imaged quasars (Narayan & Bartelmann 1999; Ehlers & Schneider 1992). For such lensed quasars that show photometric variations, it is possible to measure time delays between the lensed quasar images by cross-correlating their light curves, which in turn can be used to determine the Hubble-Lemaître constant  $H_0$  (Refsdal 1964, 1966a), which can help in constraining the dark energy equation of state (Kochanek & Schechter 2004). To date time delays of about 24 lensed quasars are known that range from a few days to a few years (Rathna Kumar et al. 2015). Measuring such time delays requires long term monitoring of lensed quasars. Among the catalogue of quasars arrived at in this work we have only identified one gravitationally lensed quasar, namely J1251+295 ( $\alpha_{2000} = 12:51:07.57$ ,  $\delta_{2000} = 29:35:40.50$ ) which has 4 lensed images with maximum angular separation of  $\sim 1.8''$  and can be easily resolved with the ILMT (the median seeing at Devasthal site is of the order of  $1.1''$ ). The ILMT will be able to provide good light curves for this source and many others. Moreover, the ILMT also expects to detect about 50 new multiply imaged quasars (Surdej et al. 2018) which opens up the ability

of the ILMT to derive more time delays among lensed quasars.

## 5. Summary

This work was aimed to arrive at a catalogue of quasars that could be used as calibrators to calibrate the ILMT observations in the world coordinate system. The details are summarized below.

1. By cross-correlating the MilliQuas catalogue with the *Gaia*-DR2, and imposing the condition of matched sources to have astrometric excess noise significance  $D \leq 2$ , we arrived at a sample of 1047747 quasars over the whole sky. Of these, 6755 quasars are available in the ILMT stripe.
2. An investigation of the distribution of proper motion for these 6755 quasars have revealed 17 sources ( $\sim 0.3\%$ ) to have a PM greater than  $20 \text{ mas yr}^{-1}$ . This confirms that quasars in the ILMT stripe have PM lesser than  $20 \text{ mas yr}^{-1}$ . As the nature of these 17 objects could not be ascertained due to the lack of optical spectra, they were excluded from our list.
3. Our final quasar catalogue for the ILMT contains 6738 quasars. Out of which, as per the MilliQuas catalogue, 2405 candidates are spectroscopically confirmed type I quasars with broad emission lines, 3 are AGN, 7 are BL Lac objects, 1 is a Type II AGN and 4322 objects are selected through photometric techniques with a probability  $> 90\%$  to be quasars. This information has been incorporated in the 8th column of our catalogue (see Table 2). The catalogue that is made available in this work, in addition to their use as astrometric calibrators, can also serve as a large sample for quasar variability studies.
4. We expect to achieve an astrometric accuracy of better than  $0.1''$  in the ILMT survey by using our proposed quasar catalogue.

## Acknowledgements

We thank the referee for her/his critical review of our manuscript. AKM and RS thank the National Academy of Sciences, India for research grant. AKM specially acknowledges the Université de Liège for providing the scholarship "Erasmus + International Credit Mobility". AKM, CSS and RS acknowledge the Alexander von Humboldt Foundation, Germany for the award of Group linkage long-term research program between

IIA, Bengaluru and European Southern Observatory, Garching, Germany. AKM and RS are thankful to the Director, IIA for providing institutional infrastructural support during this work. This research has used data from the SDSS and *Gaia*, operated by the European Space Agency.

## References

- Abolfathi B., et al., 2018, ApJS, 235, 42
- Bovy J., et al., 2011, The Astrophysical Journal, 729, 141
- Barbary, K. (2016). SEP: Source Extractor as a library. Journal of Open Source Software, 1(6), 58.
- Croom S., et al., 2004, in Mújica R., Maiolino R., eds, Multiwavelength AGN Surveys. pp 5762, doi:10.1142/9789812702432\_0015
- Ehlers J., Schneider P., 1992, Gravitational Lensing. p. 1, doi:10.1007/3-540-56180-3\_1
- Flesch E. W., 2015, Publ. Astron. Soc. Australia, 32, e010
- Flesch E. W., 2017, VizieR Online Data Catalog, p. VII/280
- Gaia Collaboration Mignard F., Klioner S., Lindegren L., Hernandez J., Bastian U., Bombrun A., 2018, Astronomy and Astrophysics, 616, A14
- Graham M., Djorgovski S. G., Stern D., Drake A. J., Mahabal A. A., Glikman E., 2016, in American Astronomical Society
- Hog, E., et al. The Tycho-2 catalogue of the 2.5 million brightest stars. NAVAL OBSERVATORY WASHINGTON DC, 2000.
- Kochanek C. S., Schechter P. L., 2004, in Freedman W. L., ed., Measuring and Modeling the Universe. p. 117 (arXiv:astro-ph/0306040)
- Kumar, B., Pandey, K. L., Pandey, S. B., Hickson, P., Borra, E. F., Anupama, G. C., & Surdej, J. (2018). The zenithal 4-m International Liquid Mirror Telescope: a unique facility for supernova studies. Monthly Notices of the Royal Astronomical Society, 476(2), 2075-2085.
- Lindegren L., et al., 2018, Astronomy and Astrophysics, 616, A2
- Lindegren L., Lammers U., Hobbs D., O'Mullane W., Bastian U., Hernández J., 2012, A&A, 538, A78
- Marrese P. M., Marinoni S., Fabrizio M., Altavilla G., 2019, A&A, 621, A144
- Myers A. D., et al., 2015, ApJS, 221, 27
- Narayan R., Bartelmann M., 1999, in Dekel A., Ostriker J. P., eds, Formation of Structure in the Universe. p. 360
- Pâris I., et al., 2018, A&A, 613, A51
- Peters C. M., et al., 2015, ApJ, 811, 95
- Rathna Kumar S., Stalin C. S., Prabhu T. P., 2015, A&A, 580, A38

- Refsdal S. 1964, MNRAS, 128, 4, p. 307-310
- Refsdal, S. 1966a, MNRAS, 132, 101
- Richards G. T., et al. 2002, AJ, 123, 2945
- Richards G. T., et al., 2009, ApJS, 180, 67
- Richards G. T., et al., 2015, VizieR Online Data Catalog, p. J/ApJS/219/39
- Ross A. J., et al., 2011, MNRAS, 417, 1350
- Sagar et al. 2000, Astron. Astrophysics Suppl. Vol 114, p. 349-362.
- Sagar, R. Kumar, B. & Omar, A. 2019 Current Science Vol. 117, p. 365
- Schmidt M., 1963, Nature, 197, 1040
- Souchay J., et al., 2015, A&A, 583, A75
- Surdej J., et al., 2018, Bulletin de la Societe Royale des Sciences de Liege, 87, 68
- Ulrich M., Maraschi L., Urry C.M., 1997, ARA&A, 35, 445
- Varshni Y. P., 1982, SScT, 521, 532
- Véron-Cetty M. P., Véron P., 2006, A&A, 455, 773
- Véron-Cetty M.-P., Véron P., 2010, A&A, 518, A10
- Wagner S.J., Witzel A., 1995, ARA&A, 33, 163